

5. H. Bernien *et al.*, *Nature* **497**, 86–90 (2013).
6. L. Rondin *et al.*, *Rep. Prog. Phys.* **77**, 056503 (2014).
7. J. J. Pla *et al.*, *Nature* **489**, 541–545 (2012).
8. K. Saeedi *et al.*, *Science* **342**, 830–833 (2013).
9. W. F. Koehl, B. B. Buckley, F. J. Heremans, G. Calusine, D. D. Awschalom, *Nature* **479**, 84–87 (2011).
10. B. B. Buckley, G. D. Fuchs, L. C. Bassett, D. D. Awschalom, *Science* **330**, 1212–1215 (2010).
11. C. G. Yale *et al.*, *Proc. Natl. Acad. Sci. U.S.A.* **110**, 7595–7600 (2013).
12. M. W. Doherty, N. B. Manson, P. Delaney, L. C. L. Hollenberg, *New J. Phys.* **13**, 025019 (2011).
13. J. R. Maze *et al.*, *New J. Phys.* **13**, 025025 (2011).
14. A. Batalov *et al.*, *Phys. Rev. Lett.* **102**, 195506 (2009).
15. P. Tamarat *et al.*, *New J. Phys.* **10**, 045004 (2008).
16. See supplementary materials on Science Online.
17. L. Marseglia *et al.*, *Appl. Phys. Lett.* **98**, 133107 (2011).
18. L. Robledo *et al.*, *Nature* **477**, 574–578 (2011).
19. N. Aslam, G. Waldherr, P. Neumann, F. Jelezko, J. Wrachtrup, *New J. Phys.* **15**, 013064 (2013).
20. G. D. Fuchs, A. L. Falk, V. V. Dobrovitski, D. D. Awschalom, *Phys. Rev. Lett.* **108**, 157602 (2012).
21. T. Hirayama, M. Sheik-Bahae, *Opt. Lett.* **27**, 860–862 (2002).
22. A. Lenef *et al.*, *Phys. Rev. B* **53**, 13427–13440 (1996).
23. K.-M. C. Fu *et al.*, *Phys. Rev. Lett.* **103**, 256404 (2009).
24. G. D. Fuchs, V. V. Dobrovitski, D. M. Toyli, F. J. Heremans, D. D. Awschalom, *Science* **326**, 1520–1522 (2009).
25. A. Gilchrist, N. K. Langford, M. A. Nielsen, *Phys. Rev. A* **71**, 062310 (2005).
26. L. C. Bassett, F. J. Heremans, C. G. Yale, B. B. Buckley, D. D. Awschalom, *Phys. Rev. Lett.* **107**, 266403 (2011).
27. D. M. Toyli, C. D. Weis, G. D. Fuchs, T. Schenkel, D. D. Awschalom, *Nano Lett.* **10**, 3168–3172 (2010).
28. A. Faraon *et al.*, *New J. Phys.* **15**, 025010 (2013).
29. J. J. Garcia-Ripoll, P. Zoller, J. I. Cirac, *Phys. Rev. Lett.* **91**, 157901 (2003).
30. M. J. Madsen *et al.*, *Phys. Rev. Lett.* **97**, 040505 (2006).
31. G. Romero, D. Ballester, Y. M. Wang, V. Scarani, E. Solano, *Phys. Rev. Lett.* **108**, 120501 (2012).

## ACKNOWLEDGMENTS

We thank K. Ohno for help with sample characterization and A. Falk for thoughtful comments. We gratefully acknowledge support from the Air Force Office of Scientific Research, the NSF DMR-1306300, and the German Research Foundation (SFB 767). All data described in this Report are presented in the supplementary materials.

## SUPPLEMENTARY MATERIALS

www.sciencemag.org/content/345/6202/1333/suppl/DC1  
Materials and Methods  
Supplementary Text  
Figs. S1 to S19  
Tables S1 to S4  
References (32–39)

2 May 2014; accepted 23 July 2014  
Published online 14 August 2014;  
10.1126/science.1255541

## MAGNETISM

# All-optical control of ferromagnetic thin films and nanostructures

C.-H. Lambert,<sup>1,2</sup> S. Mangin,<sup>1,2\*</sup> B. S. D. Ch. S. Varaprasad,<sup>3</sup> Y. K. Takahashi,<sup>3</sup> M. Hehn,<sup>2</sup> M. Cinchetti,<sup>4</sup> G. Malinowski,<sup>2</sup> K. Hono,<sup>3</sup> Y. Fainman,<sup>5</sup> M. Aeschlimann,<sup>4</sup> E. E. Fullerton<sup>1,5\*</sup>

The interplay of light and magnetism allowed light to be used as a probe of magnetic materials. Now the focus has shifted to use polarized light to alter or manipulate magnetism. Here, we demonstrate optical control of ferromagnetic materials ranging from magnetic thin films to multilayers and even granular films being explored for ultra-high-density magnetic recording. Our finding shows that optical control of magnetic materials is a much more general phenomenon than previously assumed and may have a major impact on data memory and storage industries through the integration of optical control of ferromagnetic bits.

The dynamic response of magnetic order to ultrafast external excitation is a fascinating issue of modern magnetism (1, 2). Optical probing at the femtosecond time scale allows the investigation of ultrafast magnetization dynamics, including fundamental interactions between spins, electrons, and lattice degrees of freedom far from equilibrium (1, 3–5). It further has the potential for new technologies such as heat-assisted magnetic recording (HAMR) (6, 7). An important outcome from studies of ultrafast dynamics of magnetic systems is the demonstration that circularly polarized light can directly switch magnetic domains in ferrimagnetic GdFeCo alloy films without an applied magnetic field (8). This deterministic magnetization switching using circularly polarized laser pulses is

referred to as all-optical helicity-dependent switching (AO-HDS).

Until now, ferrimagnets have been the only materials to show AO-HDS. Whereas initial studies focused on rare-earth transition-metal (RE-TM) GdFeCo alloys, there have been recent examples of AO-HDS in other RE-TM materials (9, 10), as well as synthetic ferrimagnets (11). In all cases, AO-HDS was observed for ferrimagnetic systems with two distinct sublattices that are antiferromagnetically exchange-coupled. Models for AO-HDS were based on the existence of an effective field created by the circular polarized light via the inverse Faraday effect (12, 13) or by the transfer of angular momentum from the light to the magnetic system (14). More recent models have been focused on the formation of a transient ferromagnetic state (15) due to different demagnetization times for RE and TM sublattices where the light's helicity plays a secondary role (16–18). There is also emerging evidence that laser-induced superdiffusive spin currents can flow in heterogeneous systems (18–22), potentially contributing to the AO-HDS process (18). An open question is whether AO-HDS is specific to a subset of ferrimagnetic materials or can be applied to ferromagnetic materials. Furthermore, can optical pulses also control tech-

nologically important high-anisotropy granular or patterned materials that are anticipated for future high-density magnetic recording (23)?

The optical response of ferromagnetic samples are studied by a combination of optical- and heat-assisted magnetic switching experiments where the samples are excited by a ~100-femtosecond pulsed laser source and subsequently imaged in a Faraday microscope (fig. S1). Figure 1 shows images of [Co(0.4 nm)/Pt(0.7)]<sub>N</sub> multilayers, where *N* is the number of bilayer repeats in the multilayer structure (*N* = 8, 5, and 3 repeats), which have perpendicular magnetic anisotropy, so the magnetization easy axis is normal to the film and the image contrast results from the two possible directions of the magnetization. The laser helicity is either of two circular polarizations ( $\sigma^+$  or  $\sigma^-$ ) or linear polarized (L). For Fig. 1, A to C, the laser is scanned across a region of the films that has both magnetization directions, allowing the effect of the initial state of the magnetization on the magneto-optical response to be studied.

For *N* = 8 repeats (Fig. 1A), domain formation is observed in the region scanned by the laser that is filled with disordered stripe subdomains that minimize the dipole energy (24). This process is independent of the light polarization and represents laser-induced thermal demagnetization (TD). A rim is observed at the edge of the scanned area where the magnetic orientation is opposite the background stabilized by dipolar fields from the surrounding film. For *N* = 5 repeats (Fig. 1B), the formation of subdomains in the scanned region is again observed. The average domain size is larger for decreasing number of layers, since in the thin-film limit the equilibrium domain size increases with decreasing film thickness (24). More important, the resulting domain structure depends on the light polarization. For  $\sigma^+$  light, white isolated bubble-like domains are observed in a dark background, whereas for  $\sigma^-$  light, dark domains are seen in a white background and the magnetization near the edges of the line scan favors the direction opposite the surrounding film.

In contrast, for *N* = 3 repeats (Fig. 1C), fully deterministic magnetization reversal is observed

<sup>1</sup>Center for Magnetic Recording Research, University of California San Diego, La Jolla, CA 92093-0401, USA. <sup>2</sup>Institut Jean Lamour, UMR CNRS 7198–Université de Lorraine–BP 70239, F-54506 Vandœuvre, France. <sup>3</sup>Magnetic Materials Unit, National Institute for Materials Science, Tsukuba 305-0047, Japan. <sup>4</sup>Department of Physics and Research Center OPTIMAS, University of Kaiserslautern, Erwin Schroedinger Strasse 46, 67663 Kaiserslautern, Germany. <sup>5</sup>Department of Electrical and Computer Engineering, University of California San Diego, La Jolla, CA 92093-0401, USA.

\*Corresponding author. E-mail: stephane.mangin@univ-lorraine.fr (S.M.); efullerton@ucsd.edu (E.E.F.)

for both circular polarizations that is independent of the initial magnetization direction, a clear demonstration of AO-HDS in a ferromagnetic material. The random domains created for linear polarization are much larger for  $N = 3$  repeats, in accord with the small dipolar energy gain for ultrathin films. Figure 1D shows images for the  $N = 3$  repeats sample for various laser powers where the film is saturated in one direction and the laser spot is fixed and not scanned on the surface. For low power (362 nW), a reversed domain is written for  $\sigma^+$ , there is no change to the film for  $\sigma^-$ , and a region of random domains is observed for linear polarization. With increasing laser power, regions of demagnetized random domains develop in the center of the laser spot for all three polarizations, indicating that the power is such that the temperature exceeds a critical temperature for which domains are formed (e.g., the Curie temperature  $T_C$ ). For  $\sigma^+$ , there is a rim at the edge of the demagnetized area that shows deterministic switching that is not present for  $\sigma^-$  or linearly polarized light.

We explored the effective driving energy for AO-HDS and domain formation (TD) by adding external magnetic fields to the experiments shown in Fig. 1, A to C (figs. S2 to S4). Although linear polarization leads to domain formation in zero applied field, the application of a magnetic field can stabilize a uniform magnetization state. This field increases from 3 to 4 Oe for  $N = 3$  repeats, to  $\sim 12$  Oe for  $N = 5$  repeats and  $\sim 40$  Oe for  $N = 8$  repeats, demonstrating the increased dipolar energy with thickness. When the applied field is combined with circular polarization, the applied field can either support or oppose the circular polarization. For  $N = 3$  repeats, a field of 7 Oe opposes the circular polarized light and yields a demagnetized film, whereas a field of  $\sim 12$  Oe will saturate the film in the opposite direction as that expected for the helicity of the light (fig. S4). For  $N = 5$  repeats, the field needed to yield a demagnetized film is  $\sim 12$  Oe, whereas a field of  $\sim 25$  Oe is needed to saturate the film opposite to the light helicity (fig. S3). However, when comparing the effects of circular polarization of the light to the applied magnetic field, one has to remember that the magnetic field is applied during the entire thermal process, whereas the role of the helicity of the pulse is believed to persist only for a few picoseconds after the laser excitation (25).

To determine how general AO-HDS is, we studied a range of ferromagnetic film materials, including  $[\text{Co}(t_{\text{Co}})/\text{Pt}(t_{\text{Pt}})]_N$ ,  $[\text{Co}(t_{\text{Co}})/\text{Pd}(t_{\text{Pd}})]_N$ ,  $[\text{Co}_x\text{Ni}_{1-x}(0.6 \text{ nm})/\text{Pt}(0.7 \text{ nm})]_N$ , and  $[\text{Co}/\text{Ni}]_N$  multilayer structures, where we have varied several material parameters ( $t_{\text{Co}}$ ,  $t_{\text{Pt}}$ ,  $N$ , and Ni concentration) that change materials' magnetic properties, such as magnetization,  $T_C$ , anisotropy, and exchange. AO-HDS is observed in all these ferromagnetic materials classes, including single Co layers sandwiched between Pt layers. Figure 2 summarizes selected results for the threshold laser power needed to achieve either AO-HDS (solid symbols) or TD (open symbols). For  $[\text{Co}(t_{\text{Co}})/\text{Pt}(0.7 \text{ nm})]_N$  multilayers, the results (Fig. 2A) show

AO-HDS for  $N = 2$  or 3 repeats and  $t_{\text{Co}} \leq 0.6 \text{ nm}$  (i.e., the thinnest samples) and TD for thicker samples (consistent with Fig. 1). The threshold laser power increases linearly with both  $N$  and  $t_{\text{Co}}$ , and these trends are independent of AO-HDS or TD final states. For  $[\text{Co}(0.4 \text{ nm})/\text{Pt}(t_{\text{Pt}})]_2$  samples (Fig. 2B), the threshold power decreases slightly with increasing Pt thickness. For  $N = 1$  trilayer structures—i.e.,  $\text{Pt}/\text{Co}(t_{\text{Co}})/\text{Pt}$  (Fig. 2C)—we observed AO-HDS for  $0.6 \text{ nm} \leq t_{\text{Co}} \leq 1.5 \text{ nm}$ . The upper limit is set by the thickness at which the sample maintains perpendicular magnetic anisotropy and the lower limit by the sensitivity of the optical detection. The threshold power increases linearly with  $t_{\text{Co}}$ , and the values for single Co layers are consistent with the extrapolation of the data in Fig. 2A to  $N = 1$  repeats. For  $[\text{Co}_{1-x}\text{Ni}_x(0.6 \text{ nm})/\text{Pt}(0.7 \text{ nm})]_N$  multilayers as a function of both  $N$  and Ni concentration (Fig. 2D), the threshold power increases with  $N$  as seen in Fig. 2A and decreases with Ni concentration. Finally, AO-HDS is seen for a  $\text{Cu}(10 \text{ nm})/[\text{Ni}(0.5 \text{ nm})/\text{Co}(0.1 \text{ nm})]_2/\text{Ni}(0.5 \text{ nm})/\text{Cu}(5 \text{ nm})$  multilayer.

These results show that AO-HDS is a rather general phenomenon for ferromagnetic films but is limited according to the thin-film limit, which

is useful in a number of spintronic applications (e.g., magnetic random access memory). Applications such as high-density magnetic recording require small magnetic grains or patterned bits with high magnetic anisotropy ( $K_U$ ) to remain thermally stable at the nanoscale (26). The current challenge is that the applied magnetic fields required to write high-anisotropy grains is above what can be achieved by electromagnetic write heads. HAMR is the leading technology to address the challenge when a laser spot heats the magnetic material close to  $T_C$ , allowing the magnetization to be written with a modest applied magnetic field (6, 7). We studied the role of AO-HDS in combination with applied magnetic fields on high-anisotropy FePt-based HAMR media (27). The media are FePtAgC and FePtC granular films that form high-anisotropy FePt grains separated by C grain boundaries. The average grain size is  $\sim 9.7$  and  $\sim 7.7 \text{ nm}$  for the FePtAgC and FePtC, respectively (fig. S5). The room-temperature magnetic anisotropy and coercive fields are 7 T and 3.5 T, respectively (fig. S6). Figure 3 are optical results on the FePtAgC granular film, which is initially in a random magnetic state with equal up- or down-oriented magnetic grains. Because the grain size is well below the resolution of the Faraday

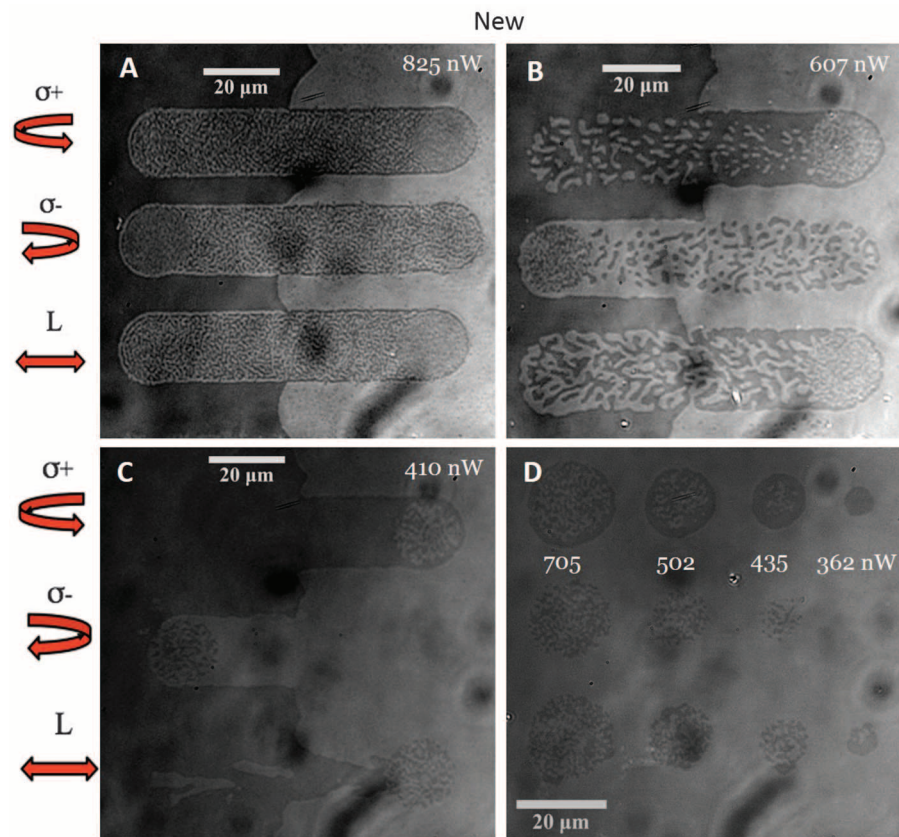


**Fig. 1. Magneto-optical response in zero applied magnetic field of  $[\text{Co}(0.4 \text{ nm})/\text{Pt}(0.7 \text{ nm})]_N$  multilayer samples to various laser polarizations.** (A)  $N = 8$  repeats. (B)  $N = 5$  repeats. (C and D)  $N = 3$  repeats. For each image, the laser is circularly polarized ( $\sigma^+$  or  $\sigma^-$ ) or linear polarized (L). For (A) to (C), the laser beam was swept over a region of the sample with two perpendicularly oriented magnetic domains showing black/white contrast in the images, with a domain wall that runs vertically in the middle of each image. In (D), the laser was fixed at individual spots over a region of the sample with uniform magnetization (white contrast). The average laser intensity at different spots is indicated in the image.



microscope, the randomly magnetized sample appears gray. Figure 3A shows that there is a net magnetization achieved that depends on the helicity of the circularly polarized light, whereas no change is observed with linear polarization. This clearly demonstrates that the film magnetization is controlled by the polarization of the light. Figure 3B shows images recorded without scanning the laser beam as in Fig. 1D. With increasing power above the threshold power (~420 nW,) there is a region of reversed grains. Above ~600 nW, a ring forms where AO-HDS occurs at a particular radius, consistent with a relatively narrow range of powers to achieve AO-HDS. The center of the ring, where the laser intensity is the highest, is demagnetized (TD-behavior), presumably exceeding  $T_C$ .

While AO-HDS is observed, the degree of magnetization is less than 100%. By comparing the contrast to the saturated film, the estimate of the induced magnetization is ~10 to 20% of saturation. The lack of saturation can arise from at least two effects. The first is that AO-HDS is only affecting a subset of the grains. The second, and more likely, is that the magnetic grains are highly thermally activated. Near  $T_C$ , there is a strong drop in  $K_U$ , the magnetic energy stored in the grain  $K_U V$  (where  $V$  is the volume of the grain) becomes comparable to thermal energy  $k_B T$ , and the particles are superparamagnetic. During the sample cooling after the optical pulse, the grain assembly can partially demagnetize due to thermal switching of individual grains [see discussion in (28)]. This effect is further driven by the dipolar fields from the neighboring grains that support a demagnetized ground state.

To quantify the role of thermal activation on AO-HDS, an external magnetic field was applied while the sample was illuminated by the polarized light. Figure 4 shows the results of line scans with both circular polarizations for different external magnetic field. An applied field of ~700 Oe is sufficient to suppress the effects of the helicity of the light where no contrast is observed for  $\sigma^-$ . For  $\sigma^+$ , the contrast increases with increasing field. Similarly, we can excite the films with linear polarized light, and an applied field of ~600 Oe yields a similar optical contrast as the AO-HDS results (fig. S7). The fact that these modest fields (relative to the room-temperature coercive field) are sufficient to magnetize the sample and/or counter the polarization of the light indicates that the sample is heated by the laser near  $T_C$ . Moreover, the grains are highly thermally activated during the optical excitation, because an external field up to 1100 Oe is not sufficient to fully saturate the film.

Our results show that AO-HDS is not exclusive to ferrimagnetic materials, and therefore antiferromagnetic exchange coupling between two magnetic sublattices is not required. Given that we observe AO-HDS switching on single Co films as well as Co/Pt and Co/Ni multilayers, it is unlikely that super-diffusive currents that couple different magnetic regions in a heterogeneous sample are required. The results do suggest that heating near the Curie point is important for the AO-HDS

in ferromagnetic materials, because the threshold intensities for both AO-HDS and TD (Fig. 2) generally track with the expected trends for  $T_C$  and do not scale with parameters such as interlayer exchange or anisotropy. Near  $T_C$ , the inverse Faraday effect or transfer of angular momentum from the light to the magnetic system is expected to be most effective. Recent modeling within the Landau-Lifshitz-Bloch formalism finds that achieving a nearly quenched magnetization is crucial for linear reversal under an ultrashort optomagnetic field pulse arising from the inverse Faraday effect (29). Well below  $T_C$ , the

magnetization reversal is precessional and governed by the Landau-Lifshitz-Gilbert equation. In the current geometry, the optomagnetic field is parallel to the magnetization, the least efficient for precessional switching (30). Similarly, when approaching  $T_C$ , the transfer of the relatively modest angular momentum in the light can lead to a symmetry breaking such that magnetization is deterministically switched.

The final ingredient for AO-HDS is that the magnetization state, once switched near  $T_C$ , be maintained while the sample cools. If demagnetization and thermal energies are too large, then

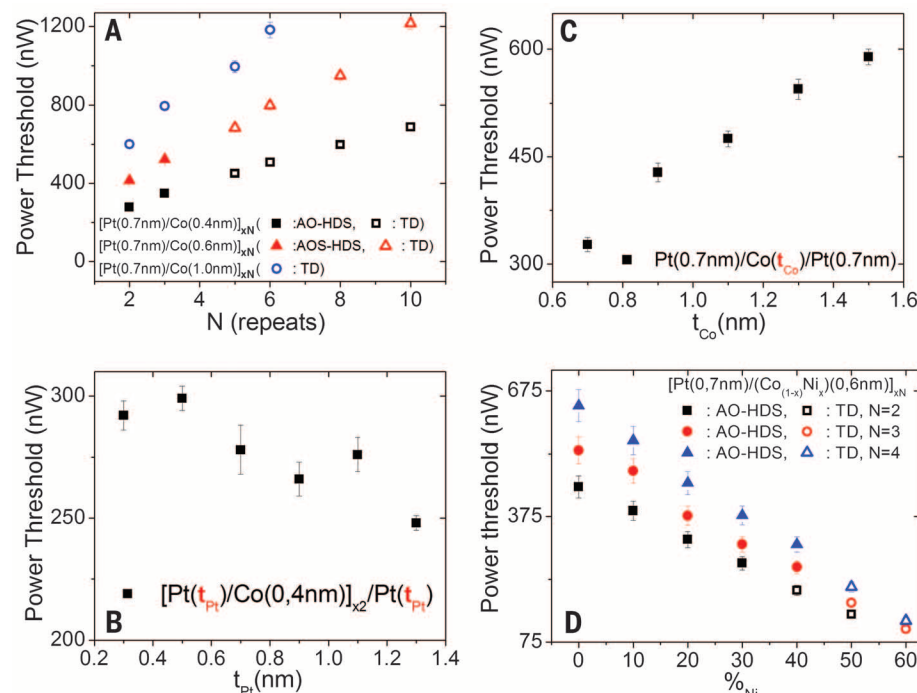


**Fig. 2. Magneto-optical response of multilayer thin-film samples to circular polarization light and varying powers.** Plotted is the evolution of the threshold power to achieve either TD or AO-HDS of various samples. For each sample, the threshold power is given either as a filled symbol for AO-HDS or open symbols for TD. (A) Threshold power versus  $N$  for  $[\text{Co}(t_{\text{Co}})/\text{Pt}(0.7 \text{ nm})]_N$  samples with  $t_{\text{Co}} = 0.4, 0.6$  and  $1.0 \text{ nm}$ . (B) Threshold power versus  $t_{\text{Pt}}$  for  $[\text{Co}(0.4 \text{ nm})/\text{Pt}(t_{\text{Pt}})]_2$  multilayer samples. (C) Threshold power versus  $t_{\text{Co}}$  for  $\text{Pt}/\text{Co}(t_{\text{Co}})/\text{Pt}$  trilayer samples. (D) Threshold power versus Ni concentration for  $[\text{Co}_{1-x}\text{Ni}_x(0.6 \text{ nm})/\text{Pd}(0.7 \text{ nm})]_N$ , with  $N = 2, 3$  or  $4$  repeats.

**Fig. 3. Magneto-optical response in zero applied magnetic field of a 15-nm FePtAgC granular film sample starting with an initially demagnetized sample.** (A) Line scans for  $\sigma^+$ ,  $\sigma^-$ , and linear polarized light (L). The laser beam was swept over the sample, and the magnetization pattern was subsequently imaged. (B) Images of magnetic domains written by keeping the laser spot at a fixed position on the sample. The laser was either  $\sigma^+$  polarized (left column) or  $\sigma^-$  polarized (right column). The laser power is given next to the image.

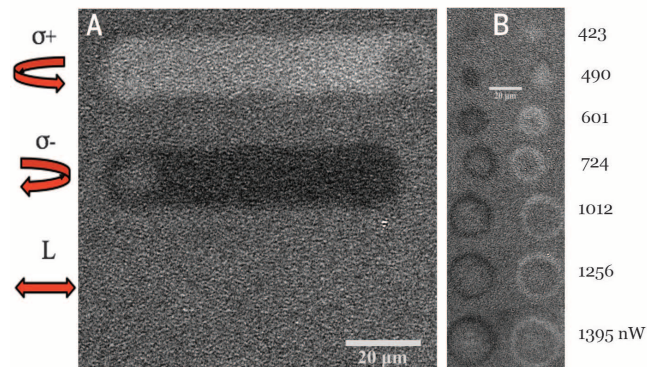
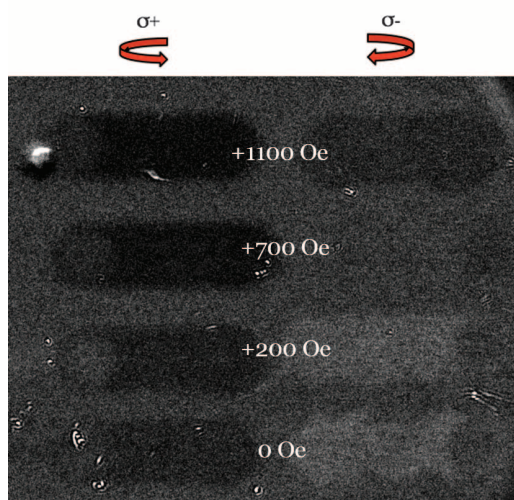


**Fig. 4. Magneto-optical response in various applied magnetic field of a 15-nm FePtAgC granular film sample starting with an initially demagnetized sample.** Shown are line scans for  $\sigma^+$  circularly polarized light in the left column and  $\sigma^-$  circularly polarized light in the right column. The laser power was 677 nW. The magnitude of the external magnetic field is given in the figures, and the orientation of the field supports  $\sigma^+$  polarization and opposes the  $\sigma^-$  polarization.



the sample will demagnetize during cooling. For perpendicular magnetized films, there are strong dipolar fields within the film that support domain formation. The dipolar energy gain for domain formation is strongly suppressed in the ultrathin film limit and explains the observation of AO-HDS only in the thin-film limit (Figs. 1 and 2). Domain formation is also suppressed for low magnetization materials, consistent with AO-HDS measurements of ferrimagnetic materials (11).

The present results on ferromagnetic materials demonstrate a new and technologically important class of materials showing AO-HDS and opens new directions in integrated magneto-optical memory, data storage, and processing applications. This study further offers progress toward a better understanding of the interaction between pulsed polarized light and magnetic materials.

#### REFERENCES AND NOTES

1. B. Koopmans *et al.*, *Nat. Mater.* **9**, 259–265 (2010).
2. A. Kirilyuk, A. V. Kimel, T. Rasing, *Rep. Prog. Phys.* **76**, 026501 (2013).
3. E. Beaupaire, J. Merle, A. Daunois, J. Bigot, *Phys. Rev. Lett.* **76**, 4250–4253 (1996).
4. S. O. Mariager *et al.*, *Phys. Rev. Lett.* **108**, 087201 (2012).
5. A. Cavalleri *et al.*, *Phys. Rev. Lett.* **87**, 237401 (2001).
6. M. H. Kryder *et al.*, *Proc. IEEE* **96**, 1810–1835 (2008).
7. B. C. Stipe *et al.*, *Nat. Photonics* **4**, 484–488 (2010).
8. C. D. Stanciu *et al.*, *Phys. Rev. Lett.* **99**, 047601 (2007).
9. S. Alebrand *et al.*, *Appl. Phys. Lett.* **101**, 162408 (2012).
10. A. Hassdenteufel *et al.*, *Adv. Mater.* **25**, 3122–3128 (2013).
11. S. Mangin *et al.*, *Nat. Mater.* **13**, 286–292 (2014).
12. J. P. van der Ziel, P. S. Pershan, L. D. Malmstrom, *Phys. Rev. Lett.* **15**, 190–193 (1965).
13. A. Kirilyuk, A. V. Kimel, T. Rasing, *Rev. Mod. Phys.* **82**, 2731–2784 (2010).
14. C. D. Stanciu *et al.*, *Phys. Rev. B* **73**, 220402 (2006).
15. I. Radu *et al.*, *Nature* **472**, 205–208 (2011).
16. T. A. Ostler *et al.*, *Nat. Commun.* **3**, 666 (2012).
17. J. H. Mentink *et al.*, *Phys. Rev. Lett.* **108**, 057202 (2012).
18. C. E. Graves *et al.*, *Nat. Mater.* **12**, 293–298 (2013).
19. E. Turgut *et al.*, *Phys. Rev. X* **3**, 039901 (2013).
20. E. Turgut *et al.*, *Phys. Rev. Lett.* **110**, 197201 (2013).
21. M. Battiato, K. Carva, P. M. Oppeneer, *Phys. Rev. Lett.* **105**, 027203 (2010).
22. G. Malinowski *et al.*, *Nat. Phys.* **4**, 855–858 (2008).
23. B. Varaprasad, M. Chen, Y. K. Takahashi, K. Hono, *IEEE Trans. Magn.* **49**, 718–722 (2013).
24. O. Hellwig, A. Berger, J. B. Kortright, E. E. Fullerton, *J. Magn. Mater.* **319**, 13–55 (2007).

25. S. Alebrand, A. Hassdenteufel, D. Steil, M. Cinchetti, M. Aeschlimann, *Phys. Rev. B* **85**, 092401 (2012).
26. A. Moser *et al.*, *J. Phys. D Appl. Phys.* **35**, R157–R167 (2002).
27. L. Zhang, Y. K. Takahashi, K. Hono, B. C. Stipe, J. Y. Juang, M. Grobis, L1<sub>0</sub>-ordered FePtAg-C granular thin film for thermally assisted magnetic recording media. *J. Appl. Phys.* **109**, 07B703 (2011).
28. H. J. Richter, A. Lyberatos, U. Nowak, R. F. L. Evans, R. W. Chantrell, *J. Appl. Phys.* **111**, 033909 (2012).

29. K. Vahaplar *et al.*, *Phys. Rev. B* **85**, 104402 (2012).
30. C. H. Back *et al.*, *Science* **285**, 864–867 (1999).

#### ACKNOWLEDGMENTS

We thank R. Tolley and M. Gottwald for help on sample fabrication and M. Menarini and V. Lomakin for helpful discussions. This work was supported by the Agence Nationale de la Recherche (ANR), ANR-10-BLANC-1005 “Friends,” and work at University of California San Diego was supported by the Office of Naval Research (ONR) Multidisciplinary University Initiative (MURI) program and a grant from the Advanced Storage Technology Consortium. It was also supported by the Partner University Fund “Novel Magnetic Materials for Spin Torque Physics” as well as the European Project (OP2M FP7-IOF-2011-298060) and the Region Lorraine. Work at the National Institute for Materials Science was supported by Advanced Storage Technology Consortium. Author contributions include the following: S.M., M.A., M.C., Y.S., and E.E.F. designed and coordinated the project; C.-H.L. grew, characterized, and optimized the thin films samples, while B.S.D.Ch.S.V., Y.K.T., and K.H. developed and grew the FePt-based granular media. C.-H.L., S.M., and Y.K.T. operated the Kerr microscope and the pump laser experiment. S.M. and E.E.F. coordinated work on the paper with contributions from C.-H.L., M.H., M.C., and G.M., with regular discussions with all authors.

#### SUPPLEMENTARY MATERIALS

www.sciencemag.org/content/345/6202/1337/suppl/DC1  
Materials and Methods  
Supplementary Text  
Figs. S1 to S7  
References

17 March 2014; accepted 4 August 2014  
Published online 21 August 2014;  
10.1126/science.1253493

#### SOCIAL PSYCHOLOGY

## Morality in everyday life

Wilhelm Hofmann,<sup>1\*</sup> Daniel C. Wisneski,<sup>2</sup> Mark J. Brandt,<sup>3</sup> Linda J. Skitka<sup>2</sup>

The science of morality has drawn heavily on well-controlled but artificial laboratory settings. To study everyday morality, we repeatedly assessed moral or immoral acts and experiences in a large ( $N = 1252$ ) sample using ecological momentary assessment. Moral experiences were surprisingly frequent and manifold. Liberals and conservatives emphasized somewhat different moral dimensions. Religious and nonreligious participants did not differ in the likelihood or quality of committed moral and immoral acts. Being the target of moral or immoral deeds had the strongest impact on happiness, whereas committing moral or immoral deeds had the strongest impact on sense of purpose. Analyses of daily dynamics revealed evidence for both moral contagion and moral licensing. In sum, morality science may benefit from a closer look at the antecedents, dynamics, and consequences of everyday moral experience.

How people distinguish between actions that are “right” and “wrong” affects many important aspects of life. Morality science—informed by philosophy, biology, anthropology, and psychology—seeks to understand how the moral sense develops (1, 2), how moral judgments are made (3, 4), how moral experiences differ among individuals, groups, and cultures (5–8), and what the psychological implications of the morally “good” or “bad” life are (9).

Insights from contemporary morality research have mostly been gained through the analysis of

moral vignettes, questionnaire data, and thought experiments such as trolley problems (10). As important as these approaches are, they are all limited to some extent by the artificial nature of the stimuli used and the non-natural settings in which they are embedded. Despite considerable scientific and practical interest in issues of morality, virtually no research has taken morality science out of these artificial settings and directly asked people about whether and how they think about morality and immorality in the course of their everyday lived experience. Here we present an attempt to capture moral events, experiences, and dynamics as they unfold in people’s natural environments.

Using ecological momentary assessment (11), we addressed a number of fundamental key issues in scientific and public debates about morality:

<sup>1</sup>Department of Psychology, University of Cologne, 50931 Cologne, Germany. <sup>2</sup>Department of Psychology, University of Illinois, Chicago, IL 60607, USA. <sup>3</sup>Department of Social Psychology, Tilburg University, 5000, Tilburg, Netherlands.  
\*Corresponding author. E-mail: wilhelm.hofmann@uni-koeln.de

## All-optical control of ferromagnetic thin films and nanostructures

C-H. Lambert, S. Mangin, B. S. D. Ch. S. Varaprasad, Y. K. Takahashi, M. Hehn, M. Cinchetti, G. Malinowski, K. Hono, Y. Fainman, M. Aeschlimann and E. E. Fullerton

*Science* **345** (6202), 1337-1340.

DOI: 10.1126/science.1253493 originally published online August 21, 2014

### All-optical magnetic state switching

Magneto-optical memory storage media, such as hard drives, use magnetic fields to change the magnetization of memory bits, but the process is slow. Light can often reveal information about the magnetization state of a sample, such as its field direction. Lambert *et al.* show that under the right circumstances, light can also switch the magnetization state of a thin ferromagnetic film. Using light pulses instead of magnetic fields led to ultrafast data memory and data storage.

*Science*, this issue p. 1337

#### ARTICLE TOOLS

<http://science.sciencemag.org/content/345/6202/1337>

#### SUPPLEMENTARY MATERIALS

<http://science.sciencemag.org/content/suppl/2014/08/20/science.1253493.DC1>

#### REFERENCES

This article cites 29 articles, 1 of which you can access for free  
<http://science.sciencemag.org/content/345/6202/1337#BIBL>

#### PERMISSIONS

<http://www.sciencemag.org/help/reprints-and-permissions>

Use of this article is subject to the [Terms of Service](#)